Surface 2π-walls in polar free-standing smectic films

P. V. Dolganov[1)], *V. K. Dolganov, A. Fukuda*[+]

Institute of Solid State Physics of the RAS, 142432 Chernogolovka, Russia

[+]*Department of Electronic and Electrical Engineering, Trinity College, University of Dublin, Dublin 2, Ireland*

Submitted 29 April 2015

It was found that electric field in free-standing smectic films at high temperature leads to formation of unusual 2π-walls, with quite different structure from the structure of classical 2π-walls. The walls are formed by the change of molecular orientation not only along the film plane (as in usual walls) but also in smectic layers between two surfaces of the film. These walls are nuclei of surface field-induced synclinic-anticlinic transition between states with transverse and longitudinal electric polarization.

DOI: 10.7868/S0370274X15110077

Orientational ordering of the molecules in liquid crystals is the reason of the formation of various orientation defects. The most common orientational defects in external electric field are linear walls separating regions with the same direction of molecular orientation. In a nematic liquid crystal the orientational order is described by the average orientation of the long axis of the rodlike molecules, so-called **n**-director [1]. Due to equivalence of the nematic director orientations **n** and $-\mathbf{n}$, line defects are π-walls, in which the molecules turn by an angle of π across the walls. The smectic liquid-crystalline structure is formed by periodically stacked two-dimensional (2D) fluid layers. In ferroelectric Smectic-C^* (SmC^*) [2] and antiferroelectric Smectic-C_A^* (SmC_A^*) [3, 4] the long axes of molecules are tilted by an angle θ with respect to the layer normal. The projection of the long molecular axis on the layer plane defines the 2D **c**-director field that describes the azimuthal molecular orientation $\phi(r)$. Two opposite directions of the **c**-director are nonequivalent [1], which leads to appearance of 2π-walls in electric field. In usual 2π-walls in smectic films the **c**-director in all layers rotates synchronously by an angle of 2π. In the direction normal to the film the structure of the wall is the same as far from the wall, but only turns by some angle [5–12]. Note that in bulk samples of SmC_A^*, contrary to thin films, π-walls are mainly observed [13–15].

In the present work 2π-walls in free-standing films of antiferroelectric liquid crystal are studied. At high temperature in the same film the states with transverse (perpendicular to the tilt plane) and longitudinal (parallel to the tilt plane) electric polarization can be formed. The existence of the state with longitudinal polarization S_L at low field and the state with transverse polarization S_T in high field leads to formation of unusual 2π-walls in which the film structure and polarization change across the wall. In particular in the high-field state S_T in the walls there exist a region which possesses the structure and polarization of the low-field state S_L. The structure transition in the films induced by the electric field can occur via the broadening of this wall region.

Measurements were performed on antiferroelectric liquid crystal (S)-TFMHPBC [4], whose chemical structure is given in Fig. 1. Bulk samples of TFMHPBC have

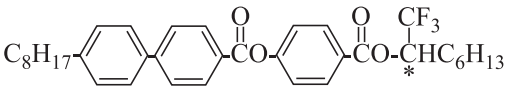

Fig. 1. Molecular structure of compound (S)-TFMHPBC

the following phase sequence: SmC_A^*–74.3 °C–SmC_α^*–75 °C–SmA–83 °C–Isotropic [4]. Films were prepared in a rectangular frame 5×0.9 mm^2 in size when the sample was in the SmC_A^* phase. Electric voltage was applied to the two longer sides of the frame. Films with thickness from 4 to 20 smectic layers were studied. The number of smectic layers N was determined by the measurements of light reflection intensity from the film [16]. 2π-walls were observed in reflected light with the use of a polarizing microscope. The image was registered by a digital camera. Films were investigated at temperatures above the SmC_α^*–SmA phase transition. In this temperature region the difference in optical path ΔnL (Δn is the difference in main indices of refraction in the plane of the film, L – its thickness) even for a 10-layer film is a small value which provides obstacles for observations with crossed polarizers. For visualization of 2π-walls the depolarized reflected light microscopy

[1)]e-mail: pauldol@issp.ac.ru

(DRLM) technique was used, which greatly enhances the contrast of the image [17]. In this method the polarization of the incident light makes an angle of 45° with respect to the direction of the electric field. The difference in indices of refraction along the **c**-director n_e and perpendicular to it n_o and correspondingly the difference in reflection coefficients leads to an effective rotation of the plane of the reflected light polarization towards the direction of the **c**-director ($n_e > n_o$). Observation of the film via a slightly decrossed analyzer enables to visualize regions with different orientation of the **c**-director in spite of the small value of ΔnL.

Antiferroelectric SmC_A^* structure becomes polar in confined geometry of thin free-standing film [18–20]. Films with an odd number of smectic layers possess transverse polarization P_T. Nonzero P_T appears since layer polarizations directed in opposite directions in neighboring layers are noncompensated in N-odd films. Films with an even number of layers possess longitudinal polarization P_L that is induced by free surfaces. This universal behavior is known as odd-even layering effect [19] and is observed in the temperature interval of the bulk SmC_A^* phase. Above the bulk transition temperature to SmA phase thin films exist in tilted state due to surface ordering effect and the high temperature shift of the surface transitions [21–23]. On heating, after a series of structure transformations a new universal behavior is observed [19, 20, 24, 25]. At high temperature film behavior in electric field does not depend on the parity of its layer number, but is determined by the value of the field. Fig. 2 shows photographs of the film in the high-field state (a) and in the low-field state (b). A difference in brightness of the film (Figs. 2a and b) is connected with different orientation of the **c**-director with respect to the electric field (vertical direction). In the DRLM geometry used for imaging the low-field structure (b) appears brighter which indicates that the orientation of the molecular tilt planes is parallel to the electric field (low-field state S_L with longitudinal polarization P_L). For the value of E above a critical field E_c, the film appears dark (a) which means that the **c**-director is perpendicular to the electric field (high-field state S_T with transverse polarization P_T).

In Fig. 3 the molecular orientation in smectic layers is shown schematically in S_L and S_T-states. At high temperature the molecules tilt mainly near the surfaces and film polarization is determined mainly by surface layers. Two types of polarization exist in the surface layers: 1) ferroelectric polarization orients perpendicular to the tilt plane (transverse polarization), 2) surface polarization is parallel to the tilt plane (longitudinal polarization). Longitudinal polarization in surface layers appears due to breaking of up-down symmetry at the air-smectic interface [18]. In S_T-structure (Fig. 3) in the lower and the upper surface layers of the film the molecules tilt in the same direction (synclinic structure, **c**-director orientation is the same). Directions of the ferroelectric transverse polarizations coincide on two surfaces. Net polarization of the film is perpendicular to the tilt plane (transverse polarization P_T). In S_L-structure (Fig. 3, the ground state without the field) in the lower and the upper surface layers the molecules tilt in the opposite directions (anticlinic structure, **c**-director orientation is the opposite). Net transverse polarization of the film is zero. Net polarization of the film is parallel to the tilt plane (longitudinal polarization P_L). Small difference of the energy between S_T and S_L-states is connected with small tilt angle θ in the middle of the film at high temperature. The transition from S_L to S_T-state on increasing field leads to the change of **c**-director orientation in surface layers and change of the type of polarization. The latter means that $P_T > P_L$. In antiferroelectric liquid crystals in high electric field the induced polarization [26, 27] can be important and can lead to a number of effects. In particular the induced po-

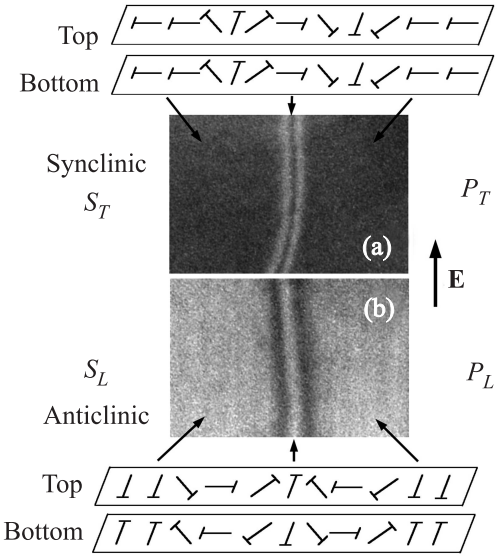

Fig. 2. Photographs of a smectic film in the high-field state (S_T) with transverse polarization (a) and in the low-field state (S_L) with longitudinal polarization (b). The transition from S_L- to S_T-state is induced by the electric field. Double dark and bright stripes are classical 2π-walls. The orientation of the **c**-director in 2π-walls in top and bottom surface layers of the film is shown schematically in S_T- and S_L-states. The orientation of surface smectic layers is synclinic in S_T (a) and anticlinic in S_L (b). The horizontal dimension of each photograph is 260 μm, number of layers $N = 11$, T=77.4 °C, $E = 5.1$ V/cm (a), $E = 3.7$ V/cm (b)

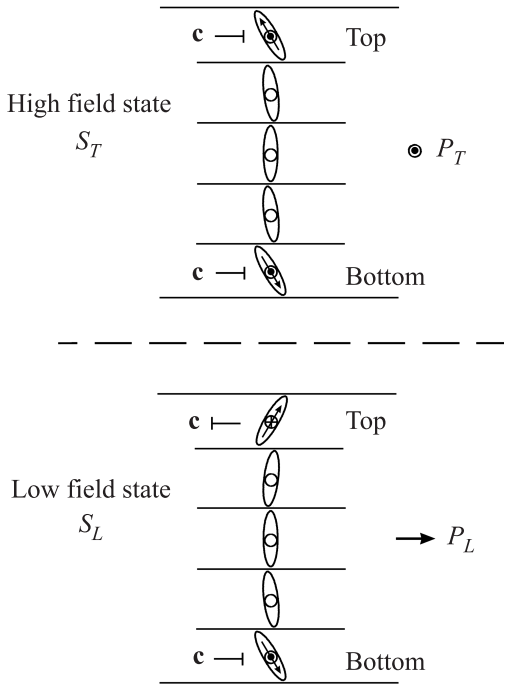

Fig. 3. Schematic representation of the film structure in S_T (high field) and S_L (low field) states. In the surface layers the directions of polarization are shown by arrows. In S_T-state the orientation of molecules in the top and bottom surface layers is the same. The surfaces are synclinic and the film possesses transverse polarization P_T. In S_L-state the orientation of molecules in top and bottom surface layers is opposite. The surfaces are anticlinic and film possesses longitudinal polarization P_L. Field-induced transition between state with longitudinal P_L and transverse P_T polarization takes place at the critical electric field E_c

larization can play an important role in pretransitional effects, helix unwinding, field-induced birefringence [27–29]. The induced polarization is parallel to the electric field and is along the tilting direction [27]. In our experiments we used values of electric field much lower than usually employed in studies of bulk antiferroelectrics, where induced polarization plays an important role. In our experiments the state with longitudinal polarization appears in the low-field state, where the contribution of the field-induced polarization is small and longitudinal polarization is mainly related with surface layers. At high field the state with transverse polarization is stable.

Double stripes in Fig. 2 are 2π-walls. Their structure is presented schematically in the Figure where orientation of the **c**-director across the walls is shown in the bottom and top layers of the films. In the centers of bright (a) and dark (b) stripes the **c**-director is oriented by an angle $\pi/2$ with respect to its orientation in the defect-free part of the sample. Walls have a classical structure similar to 2π-walls in ferroelectric and antiferroelectric phase at low temperature [5, 9]. They are formed by a continuous rotation of the **c**-director by an angle of 2π across the wall in all layers of the film, so that the interlayer structure of the walls is the same as in the defect-free part of the film, but only turns by some angles. Further we shall refer to these classical walls as W_0-walls.

Besides classical 2π-walls in the high-field state (S_T-structure), line defects of other types with unusual structures were found (Figs. 4 and 5). These defects

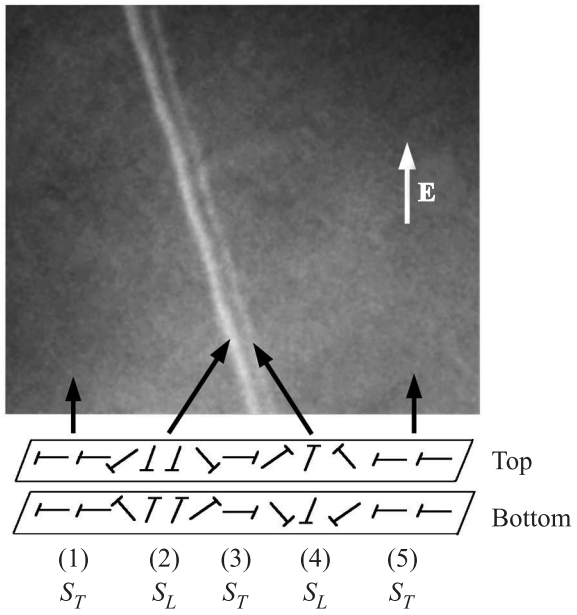

Fig. 4. Photograph of a W_1-wall in the high field state (S_T). Schematic representation of the structure of W_1-wall is shown in the lower part of the Figure. The **c**-director orientation is shown in top and bottom surface layers of the films. The **c**-director rotates in opposite directions in two surface layers. In the region *2* of the wall the structure and polarization correspond to the low-field state S_L. $E = 6\,\mathrm{V/cm}$, $T = 78.7\,^\circ\mathrm{C}$. The horizontal dimension of the image is $330\,\mu$m

we will designate as W_1- and W_2-walls, to distinguish them from classical W_0-walls. The line defects in Figs. 4 and 5, like classical 2π-walls, border regions with the same orientation of the **c**-director and in this sense they are also 2π-walls. However, structures of these walls differ essentially from classical walls observed in polar liquid crystals. W_1-wall (Fig. 4), like a W_0-wall, consists of two stripes, but their widths differ substantially. Unlike the W_0-wall depolarized reflection from the W_2-wall is triple (Fig. 5). Behavior of the walls near the field

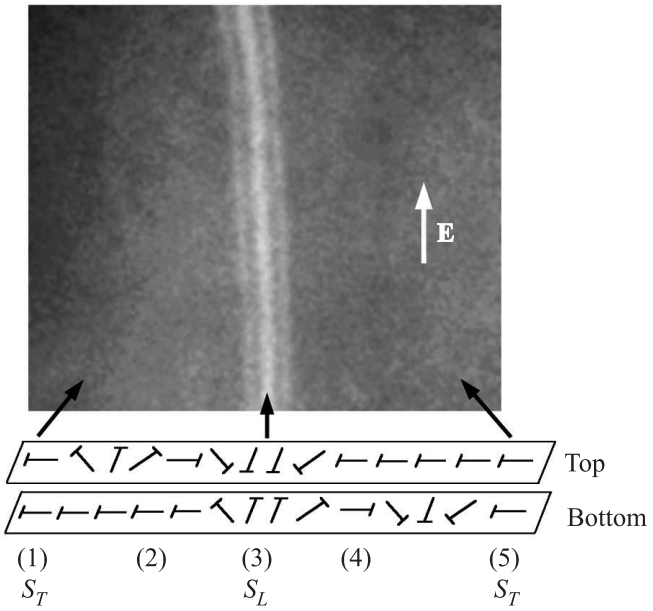

Fig. 5. Photograph of a W_2-wall in the high field state (S_T). Schematic representation of the structure of W_2-wall is shown in the lower part of the Figure. The **c**-director orientation is shown in top and bottom surface layers of the films. Two surface walls are shifted relative to each other. In the region (3) of the wall the structure and polarization correspond to low-field state S_L. $E = 9\,\mathrm{V/cm}$, $T = 78.9\,^\circ\mathrm{C}$. The horizontal dimension of the image is $220\,\mu\mathrm{m}$

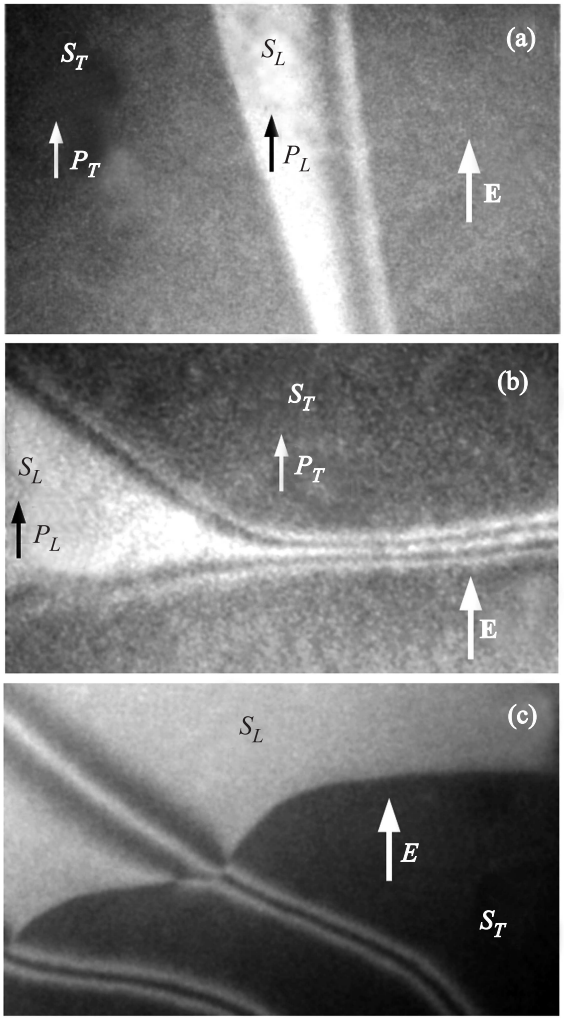

Fig. 6. Transition from the structure with transverse polarization S_T (dark region of the film) to the structure with longitudinal polarization S_L (bright region) at decreasing field. In Fig. 6a the S_L-state appears via the broadening of one of the stripes of W_1-wall (the left one in Fig. 4). In Fig. 6b the S_L-state is formed via the broadening of the middle part of W_2-wall, $E_c = 4.8\,\mathrm{V/cm}$, $T = 78.7\,^\circ\mathrm{C}$. The horizontal dimension of each image is $315\,\mu\mathrm{m}$. (c) Transition between S_T and S_L-states in the film with classical W_0-walls

E_c of the transition between S_T and S_L-states shows that the wider stripe of W_1-wall and the middle stripe of the W_2-wall possess the structure of the polar S_L-state with longitudinal ferroelectric polarization. Upon decreasing E the middle stripe of W_2-wall broadens (left side of Fig. 6b). In the newly appeared bright region the film is in the S_L-state. A similar transformation occurs with the W_1-wall. S_L-structure of macroscopic dimensions (left bright region in Fig. 6a) emerged from the wider stripe of a W_1-wall (Fig. 4) upon decreasing the electric field. So W_1- and W_2-walls act as nuclei of the transition from S_T to S_L-states. This is not the case for W_0-walls. Clear difference between W_1-, W_2-walls and W_0-walls can be seen from the comparison of the transitions in the films with W_1-, W_2-walls (Fig. 6a and b) and with W_0-walls (Fig. 6c). The transition (front between dark and bright regions) occurs in the whole sample outside the W_0-walls (Fig. 6c). At the transition the appearance of the W_0-walls also changes, bright stripes become dark and vice versa due to the structure transition in the walls, but W_0-walls are not nuclei of the transition. W_0-walls are observed in the SmC_A^* phase and at high temperature, both in the low-field state and in the high-field state (Fig. 6c). W_1- and W_2-walls were observed only at high temperature in the high-field S_T-state. W_1- and W_2-walls typically appear during the transition from S_L-state to S_T-state.

Structure of W_1- and W_2-walls may be determined by considering the microscopic model of **c**-director reorientation in smectic layers on the front of the transition from the high-field (S_T) to the low-field (S_L) state (Figs. 6a and b). The rotation of the **c**-director across W_1- and W_2-walls is shown in the lower parts of Figs. 4

and 5. In regions denoted (1) and (5) the films are in the S_T-state. In S_L- and S_T-structures the directions of the tilt planes are perpendicular to each other (Fig. 2), but the direction of electric polarization is the same (Figs. 6a and b). The most simple way of the transition from S_T- to S_L-structure consists of a rotation of the **c**-director by an angle of $\pi/2$ in opposite directions in the upper and lower surface smectic layers (Fig. 4). Such a reorientation leads to formation of S_L-structure (region *2* in Fig. 4) and change of the intensity from dark (S_T) to bright (S_L) in DRLM (left bright stripes in Figs. 4 and 6a). Further **c**-director rotation leads again to formation of the S_L-structure in the region *4*, Fig. 4. The direction of longitudinal polarization P_L coincides with P_T and with the field E in the region *2* and is opposite to P_T and E in region *4*. This is the reason of different width of the bright stripes in W_1-wall (Fig. 4). Part of the wall *2* whose longitudinal polarization P_L coincides with E is broader. At the transition $S_T \to S_L$ it further broads (Fig. 6a) and occupies the whole film.

The other way of transition from S_T to S_L-structure is shown schematically in the lower part of Fig. 5. 2π-walls in top and bottom surface layers are shifted with respect to each other. Such a shift leads to appearance of triplet structure of the W_2-wall (Fig. 5). Likewise in W_1 (and contrary to the classical W_0-wall), inside W_2 there exists a region *3* with S_L-structure and with direction of polarization P_L parallel to the electric field (the central part of the W_2-wall). Decrease of the electric field leads to broadening of the region *3* with S_L-structure (Fig. 6b) and to transition of whole film to S_L-state. Line defects similar to W_2-wall have been observed previously after transition in the electric field from nonpolar SmC to the structure with longitudinal polarization [30]. However, in the latter case the central parts of the walls correspond to nonpolar ground state and do not possess electric polarization.

It is known that two classical 2π-walls repel when the sense of the **c**-director rotation in the walls is the same and attract each other with following annihilation when the sense of the **c**-director rotation is the opposite [9]. At the borders of a W_2-wall the **c**-director rotates only in one half of the film (Fig. 5). This can lead to a specific interaction between W_2-walls. Two W_2-walls can partially overlap so that one bright stripe from each wall (two regions where the **c**-director rotates only in one half of the film, Fig. 5) adjoin together. A nontrivial stable structure which consists of 5 bright stripes is formed (Fig. 7).

Width of W_0-walls is determined by the ratio of P/K [5], where K is the $2D$ Frank elastic constant. From the relative width of the W_0-walls in S_T- and S_L-structures we can conclude that P_T is approximately two times larger than P_L. At the field-induced S_L–S_T transition the energy ε_1 of reorientation in interior layers is compensated by the electrostatic energy $\varepsilon_2 = -(P_T - P_L)E_c$. So the energy of layer reorientation ε_1 is about $P_L E_c$. Now there is no theory describing the structure of W_1- and W_2-walls. We can make only some speculations. Wall regions with S_L structure decrease the electrostatic energy since the longitudinal polarization in region *2* in Fig. 4 and *3* in Fig. 5 is parallel to E. So we may guess that the energy of the W_1- and W_2-walls may be of the order or even smaller than the energy of classical W_0-walls.

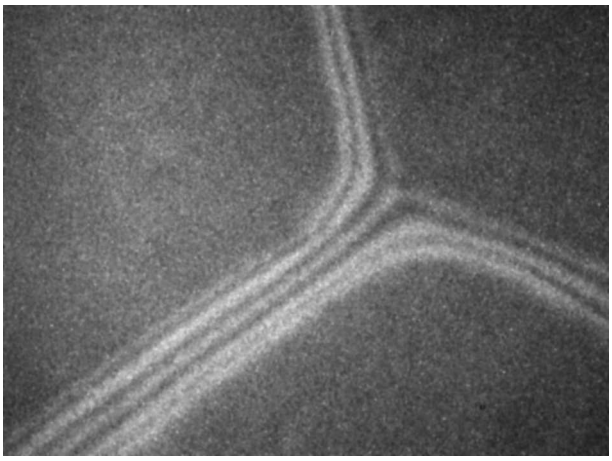

Fig. 7. Structure formed by two partly overlapping W_2-walls. $E = 10\,\mathrm{V/cm}$, $T = 78.9\,^\circ\mathrm{C}$. The horizontal dimension of the image is about $300\,\mu\mathrm{m}$

In summary, 2π-walls in polar free-standing films of liquid crystal were studied. Besides classical 2π-walls, linear defects with unusual structure can be formed. A distinguishing feature of W_1- and W_2-walls is the existence of the regions inside the walls with different structures and polarization parallel to the electric field. Such walls prompt the field-induced transition in the films.

This work was supported in part by RFBR projects # 13-02-00120, 14-02-01130, and 15-02-05706.

1. P. G. de Gennes, *The Physics of Liquid Crystals*, Clarendon, Oxford (1974); Mir, M. (1977).
2. R. B. Meyer, L. Liebert, L. Strzelecki, and P. Keller, J. Phys. (Paris) Lett. **36**, L69 (1975).
3. A. D. L. Chandani, E. Gorecka, Y. Ouchi, H. Takezoe, and A. Fukuda, Jpn. J. Appl. Phys. **28**, L1265 (1989).
4. A. Fukuda, Y. Takanishi, T. Isosaki, K. Ishikawa, and H. Takezoe, J. Mater. Chem. **4**, 997 (1994).
5. R. Pindak, C. Y. Young, R. B. Meyer, and N. A. Clark, Phys. Rev. Lett. **45**, 1193 (1980).

6. D. R. Link, L. Radzihovsky, G. Natale, J. E. Maclennan, and N. A. Clark, Phys. Rev. Lett. **84**, 5772 (2000).
7. P. V. Dolganov and B. M. Bolotin, Pis'ma v ZhETF **77**, 503 (2003) [JETP Lett. **77**, 429 (2003)].
8. R. Stannarius, J. Li, and W. Weissflog, Phys. Rev. Lett. **90**, 025502 (2003).
9. P. V. Dolganov, B. M. Bolotin, and A. Fukuda, Phys. Rev. E **70**, 041708 (2004).
10. P. V. Dolganov, V. K. Dolganov, and P. Cluzeau, Pis'ma v ZhETF **96**, 347 (2012) [JETP Lett. **96**, 317 (2012)].
11. P. V. Dolganov, V. K. Dolganov, and P. Cluzeau, JETP **116**, 1043 (2013).
12. N. Chattham, M.-G. Tamba, R. Stannarius, E. Westphal, H. Gallarda, M. Prehm, C. Tschierske, H. Takezoe, and A. Eremin, Phys. Rev. E **91**, 030502(R) (2015).
13. Y. Takanishi, H. Takezoe, A. Fukuda, and J. Watanabe, Phys. Rev. B **45**, 7684 (1992).
14. Y. Takanishi, H. Takezoe, A. Fukuda, H. Komura, and J. Watanabe, J. Mater. Chem. **2**, 71 (1992).
15. K. Miyachi, Y. Takanishi, K. Ishikawa, H. Takezoe, and A. Fukuda, Ferroelectrics **149**, 61 (1993).
16. P. Pieranski, L. Beliard, J.-Ph. Tournellec, X. Leoncini, C. Furtlehner, H. Dumoulin, E. Riou, B. Jouvin, J.-P. Fénerol, Ph. Palaric, J. Heuving, B. Cartier, and I. Kraus, Physica A **194**, 364 (1993).
17. D. R. Link, G. Natale, R. Shao, J. E. Maclennan, N. A. Clark, E. Korblova, and D. M. Walba, Science **278**, 1924 (1999).
18. D. R. Link, J. E. Maclennan, and N. A. Clark, Phys. Rev. Lett. **77**, 2237 (1996).
19. D. R. Link, G. Natale, N. A. Clark, J. E. Maclennan, M. Walsh, S. S. Keast, and M. E. Neubert, Phys. Rev. Lett. **82**, 2508 (1999).
20. P. V. Dolganov, Y. Suzuki, and A. Fukuda, Phys. Rev. E **65**, 031702 (2002).
21. S. Henekamp, R. A. Pelcovits, E. Fontes, E. Y. Chen, R. Pindak, and R. Meyer, Phys. Rev. Lett. **52**, 1017 (1984).
22. Ch. Bahr, Int. J. Mod. Phys. B **8**, 3051 (1994).
23. T. Stoebe and C. C. Huang, Int. J. Mod. Phys. B **9**, 2285 (1995).
24. P. M. Johnson, D. A. Olson, S. Pankratz, Ch. Bahr, J. W. Goodby, and C. C. Huang, Phys. Rev. E **62**, 8106 (2000).
25. P. V. Dolganov, E. I. Demikhov, Y. Suzuki, and A. Fukuda, JETP **95**, 728 (2002).
26. K. Hiraoka, H. Takezoe, and A. Fukuda, Feroelectrics **147**, 13 (1993).
27. L. A. Parry-Jones and S. J. Elston, Phys. Rev. E **63**, 050701(R) (2001).
28. T. Qian and P. L. Taylor, Phys. Rev. E **60**, 2978 (1999).
29. K. L. Sandhya, A. D. L. Chandani, A. Fukuda, S. Kumar, and J. K. Vij, Phys. Rev. E **87** 062506 (2013).
30. D. R. Link, G. Natale, J. E. Maclennan, and N. A. Clark, Phys. Rev. Lett. **83**, 3665 (1999).